# Doppler Shift Measurement Using Complex-Valued CSI of WiFi in Corridors

Dandan Yang, Tao Wang, Yanzan Sun, Yating Wu
Key laboratory of Specialty Fiber Optics and Optical Access Networks
Joint International Research Laboratory of Specialty Fiber Optics and Advanced Communication
Shanghai Institute for Advanced Communication and Data Science, Shanghai University,
Shanghai, P. R. China
e-mail: yangdd03@126.com, twang@shu.edu.cn, yanzansun@shu.edu.cn, ytwu@shu.edu.cn

*Abstract*—**This paper presents a novel approach to measure indoor Doppler shift (which is generally neglected) based on Channel State Information (CSI) using WiFi. Our approach is motivated by the fact that the CSI provided by a commercially available measurement tool is complex-valued, and therefore the Fast Fourier Transform (FFT) of CSI is not conjugate-symmetric. After establishing a CSI acquisition system, we process CSI data guided by theoretical derivation under different corridor scenarios and finally obtain the Doppler shift of different relative motions. Our results demonstrate that this method of measuring Doppler shift could be applied to further research on crowd counting or human activity recognition based on WiFi.**

***Keywords-WiFi; indoor; Doppler shift; CSI***

## I. INTRODUCTION

In recent years, wireless technologies tend to mature, and more scholars begin to pay attention to diverse applications using wireless signals. WiFi with a widely installed infrastructure has aroused great interest for its capability of sensing the channel changes introduced by human bodies.

Utilizing WiFi signal's transmission characteristics such as Received Signal Strength Indicator (RSSI) and Channel State Information (CSI), changes in environment could be captured [1]. This paves the way to intrusion detection, crowd counting, activity recognition, etc. Compared to other RF-based systems such as Bluetooth, Ultra-wideband (UWB) and Radar, WiFi-based systems have superiority for its extensive coverage, simple configuration, and low cost.

In general, WiFi-based systems could be divided into device-based approaches and device-free approaches. In this paper, we consider the device-free approach which becomes increasingly popular since target is not required to carry certain devices accessing specific network. In particular, RSSI [2-3] or CSI [4-8] is employed to measure the variances of WiFi signal. On the one hand, RSSI could be easily obtained and has been widely adopted in WiFi-based indoor positioning [9]. However, it suffers from dramatic performance degradation due to multipath fading [10-11], which poses difficulties for RSSI-based systems. On the other hand, CSI could describe channel frequency response of each subcarrier based on Orthogonal Frequency Division Multiplexing (OFDM) and it is much more robust. Not only providing more stable and reliable amplitude information than RSSI, CSI also reveals phase information. More CSI-based applications have been proposed with the release of the driver developed for Intel WiFi card 5300 [12].

This paper presents a device-free system to measure indoor Doppler shift based on CSI. It is worth noting that existing CSI-based systems only take the amplitude of CSI values for following data processing. For instance, [4] measures WiFi variances with a dilated matrix of CSI amplitude (i.e., the absolute value of complex-valued CSI), [6] also obtains Doppler spectrum with the Fast Fourier Transform (FFT) of CSI amplitude, [12] builds a CSI-based speed model by calculating the length of path based on CSI amplitude. During our previous experiments, we observed that the FFT of CSI (which is actually complex-valued) is not conjugate-symmetric, so it could reveal the velocity of detected objects more directly and efficiently. Based on this observation, we succeed in measuring indoor Doppler shift containing speed and direction of motion for further human detection.

The rest of this paper is organized as follows. Section II theoretically analyses the principle of CSI-based Doppler shift measurement. CSI acquisition system is built in Section III, followed by data processing in Section IV. In Section V, experiments are carried out in a corridor to verify the effectiveness of the theoretical analysis. Section VI concludes this paper.

## II. THEORETICAL ANALYSIS

In this section, the principle of Doppler shift measurement using CSI is discussed. To facilitate readers' understanding, important symbol definitions and meanings used in the following text are listed in Tab. I.

Suppose a transmitter and a receiver are $d$ apart at a certain instant. As shown in Fig. 1, the transmitter is continuously broadcasting WiFi signal while the receiver is moving away at velocity $v$. Therefore, WiFi signal arrives at the receiver through a time-varying and multipath channel. Assume there are $L$ separate paths in total and Fig. 1 shows two of them where $\theta_l$ denotes the angle between the arrival direction of $l$-th path and receiver's moving direction.

As channel response, CSI of $k$-th subcarrier collected at time instant $nTs$ can be expressed as:

$$h_k(nT_s) = \sum_{l=1}^{L} \alpha_l e^{-j\omega_k \frac{d_l}{c}} e^{j\omega_k \frac{v_l}{c} nT_s} + \varepsilon_k, \tag{1}$$

where $v_l$ can be expressed as:

$$v_l = v\cos\theta_l \quad (2)$$

It can be easily noticed that when the receiver moves away from the transmitter, $v_l$ is a negative value, otherwise, it is positive.

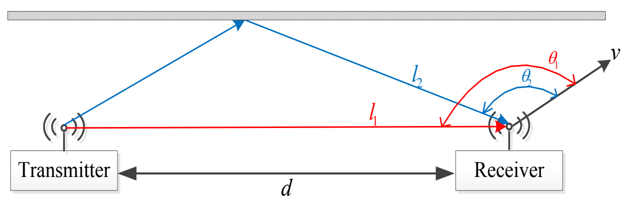


Figure 1. Illustration of the transmitter-receiver link under consideration.

TABLE I. SYMBOL DEFINITIONS AND PHYSICAL MEANINGS.

| Symbol definition | Physical meaning |
|---|---|
| $k$ | subcarrier number(30 subcarriers in total) |
| $T_S$ | time interval of CSI sampling |
| $l$ | path number(assume there are $L$ paths in total) |
| $\alpha_l$ | amplitude of $l$-th path |
| $\omega_k$ | angular frequency of $k$-th subcarrier |
| $d_l$ | length of $l$-th path |
| $c$ | velocity of electromagnetic wave($3\times10^8$m/s) |
| $v_l$ | projection of receiver's velocity in $l$-th path |
| $\varepsilon_k$ | measurement error in $k$-th subcarrier |

Since 802.11n protocol operates from 2.4GHz to 2.4835GHz [13], here we suppose WiFi signal is sent on Channel 1, i.e., the frequency of the subcarrier starts from 2.4 GHz. According to 802.11n protocol, there are 56 subcarriers within 20MHz channel, and the commercially available CSI tool used in experiments can collect CSI measurements for 30 out of 56 subcarriers. Moreover, these 30 subcarriers are allocated in the frequency band [2.4GHz, 2.42GHz] and the frequency of $k$-th subcarrier is:

$$f_k = 2.4 + k\Delta f, \qquad k = 1, 2, \ldots, 30. \quad (3)$$

where $\Delta f$ is frequency difference between subcarriers and it equals to $6.7\times10^{-4}$GHz which is quite small compared with 2.4GHz.

For the $k$-th subcarrier, the Doppler shift frequency is $\omega_k v_l / c$, which is approximately equal to

$$\omega_l = 2\pi f_l = 2\pi \times 2.4\times10^9 \frac{v_l}{c}, \quad (4)$$

since $f_k$ is almost the same for different subcarriers. Motivated by above observation, we take average of CSI of all 30 subcarriers and obtain:

$$\bar{h}(nT_s) = \frac{1}{30}\sum_{l=1}^{L}\sum_{k=1}^{30}\alpha_l e^{-j\omega_k\frac{d_l}{c}} e^{j\omega_l nT_s} + \frac{1}{30}\sum_{k=1}^{30}\varepsilon_k, \quad (5)$$

which is also beneficial to signal de-noising.

The FFT of $\bar{h}(nT_s)$ is obtained:

$$\begin{aligned}\bar{H}(m) &= \sum_{n=0}^{N-1}\bar{h}(nT_s)e^{-j(\frac{2\pi}{N})nm} \\ &= \frac{1}{30}\sum_{l=1}^{L}\sum_{k=1}^{30}\alpha_l e^{-j\omega_k\frac{d_l}{c}}\sum_{n=0}^{N-1}e^{j2\pi(f_l T_s - \frac{m}{N})n} + \frac{1}{30}\sum_{k=1}^{30}E_k,\end{aligned} \quad (6)$$

where $E_k$ is FFT of $\varepsilon_k$ and we define $\Phi_{l,m}$ as:

$$\Phi_{l,m} = \sum_{n=0}^{N-1}e^{j2\pi(f_l T_s - \frac{m}{N})n}, \quad (7)$$

then (6) can be expressed as:

$$\bar{H}(m) = \frac{1}{30}\sum_{l=1}^{L}\sum_{k=1}^{30}\alpha_l e^{-j\omega_k\frac{d_l}{c}} \cdot \Phi_{l,m} + \frac{1}{30}\sum_{k=1}^{30}E_k. \quad (8)$$

The absolute value of $\Phi_{l,m}$ would get the maximum when the following equation is satisfied:

$$f_l T_s - \frac{m}{N} = p\pi, p \in Z, \quad (9)$$

i.e. $f_l = m/NT_s + p\pi/T_s$ (the value of $p$ is related to the range of $m$). In this condition, $|\bar{H}(m)|$ can achieve the maximum value and $f_l$ is Doppler frequency required. We will show the procedure of measuring Doppler shift frequency based on the above principle in the following sections.

## III. DATA ACQUISITION

CSI could be considered as the channel response depicting the amplitudes and phases of 30 subcarriers, which makes it finer-grained and more stable. To obtain CSI values remotely, we build a CSI acquisition system as shown in Fig. 2. Laptop1 is placed outside the test space as the overall console of the system while Laptop2 and WiFi router are placed inside to collect CSI values. The layout could avoid interference on wireless channel from human's operation on Laptop1. Laptop1 receives CSI values obtained in Laptop2 through TCP/IP protocol and performs data processing with Matlab.

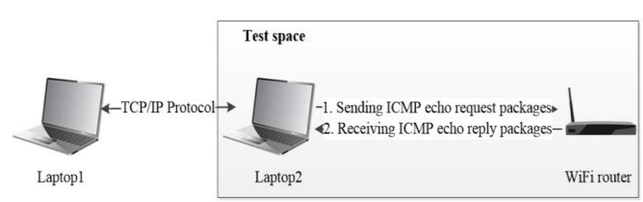


Figure 2. Our CSI acquisition system.

The hardware and software configured in our system are shown in Tab. 2 and Fig. 3.

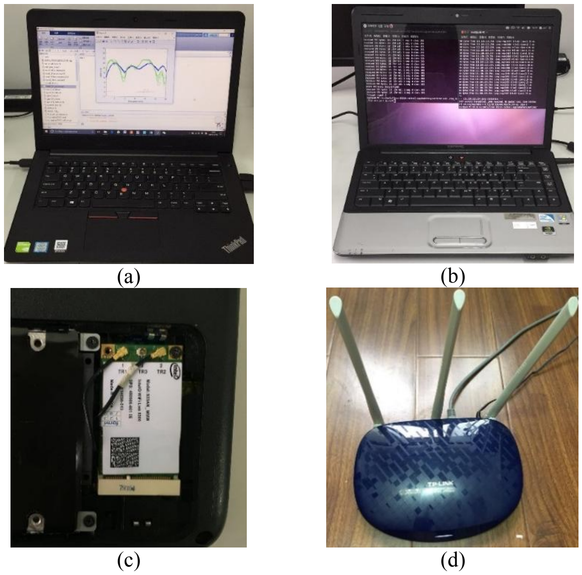


Figure 3. Devices.

TABLE II. HARDWARE AND SOFTWARE CONFIGURATION.

| Label | Hardware | Software | Figure |
|---|---|---|---|
| Laptop1 | ThinkPad E470 | Matlab 2016a | Fig. 3 (a) |
| Laptop2 | HP Presario CQ40, Intel WiFi 5300 | Ubuntu 11.04, Linux 802.11n, CSI Tool | Fig. 3(b)(c) |
| WiFi router | TP-Link TL-WR886N | / | Fig. 3(d) |

## IV. DATA PROCESSING

Since the CSI acquisition system is a Multiple Input Multiple Output (MIMO) system, suppose that there are $M$ transmit antennas and $N$ receive antennas, then there are $N_{ch}=M\times N$ WiFi links. In each link, 30 of 56 subcarriers are sampled and the number of packages increases as time goes on. The CSI values in $n$-th link could be expressed as a $30\times p$ complex matrix:

$$h^n = \begin{bmatrix} h^n_{1,1} & \cdots & h^n_{1,j} & \cdots & h^n_{1,p} \\ \vdots & \ddots & \vdots & \ddots & \vdots \\ h^n_{i,1} & \cdots & h^n_{i,j} & \cdots & h^n_{i,p} \\ \vdots & \ddots & \vdots & \ddots & \vdots \\ h^n_{30,1} & \cdots & h^n_{30,j} & \cdots & h^n_{30,p} \end{bmatrix}, \tag{10}$$

where $h^n_{i,j}$ is the CSI value in the $i$-th subcarrier, $j$-th package and the $n$-th link. As shown in Fig. 4, we could observe that not only different multipath propagation scenarios would result in changes in CSI values(from Fig. 4(a),(b)), but also different relative motions between the transmitter and receiver could cause dramatic changes in CSI amplitude (from Fig. 4(c),(d)).

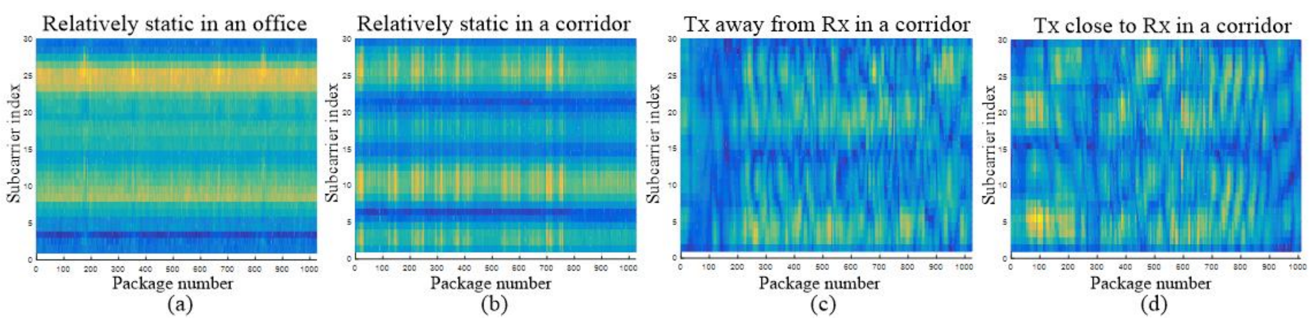


Figure 4. CSI amplitude in different channel environment.

According to the theoretical analysis in Section II, Doppler frequency could be obtained by following two steps:

1) Our system could support 3×3=9 links in total, we choose the first one and average each column:

$$\begin{aligned} \overline{h^1} &= \frac{1}{30}\sum_{i=1}^{30}\left[h^1_{i,1} \;\cdots\; h^1_{i,j} \;\cdots\; h^1_{i,p}\right], \\ &= \left[h^1_1 \;\cdots\; h^1_j \;\cdots\; h^1_p\right] \end{aligned} \tag{11}$$

where $h^1_j$ is the mean CSI value of all 30 subcarriers in the $j$-th package and 1st link.

2) The FFT of the mean CSI value is computed over a sliding window of size $W$:

$$\overline{H_k^1}(j_0) = \left|\sum_{j=j_0+1}^{j_0+W} \overline{h^1}\cdot \mathrm{e}^{-\sqrt{-1}\frac{2\pi}{W}jk}\right|, k = 1,2,\ldots W \tag{12}$$

Subsequently, we could obtain a matrix which contains the Doppler frequency:

$$\overline{H^1}(j_0) = \left[H_1^1(j_0) \;\cdots\; H_k^1(j_0) \;\cdots\; H_W^1(j_0)\right]. \tag{13}$$

The frequency with maximum amplitude is Doppler frequency required.

## V. Experiment Results

In this section, we conduct experiments to verify the correctness of theoretical deduction in Section II.

The experiments are conducted in a corridor (3m × 10m) as shown in Fig. 5. The WiFi Router is Tx and Laptop2 is Rx as marked in the figure. During the whole experiment, Rx could move between the location in the figure (10m away from Tx) and Tx. Laptop1, the data processing center, is fixed 1m out of the test area to enable the stable TCP/IP transmission with Laptop2.

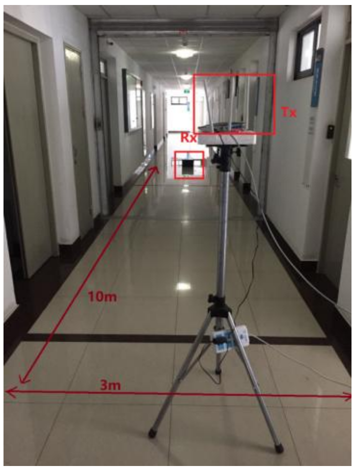


Figure 5. Experiment scene.

Experiments are performed to measure the Doppler frequency under 3 cases:

- *Case 1*: Tx and Rx keep static as shown in Fig. 5.
- *Case 2*: Rx (held by a person) moved toward Tx at about 1m/s.
- *Case 3*: Starting from the location of Tx, Rx (held by a person) moved away at about 1m/s.

We intercept 512 packages of each case considering the sampling rate of CSI and duration of each case, then obtain 3 CSI matrixes (30×512). Each matrix is processed following the steps in Section IV and the size of the sliding window $W$ is 512. The final results are shown in Fig. 6.

Theoretically, when the speed of relative motion is 1m/s, it could be calculated that Doppler shift of WiFi signal is about 8Hz. When the receiver is relatively close to transmitter, Doppler frequency is positive, otherwise, it is negative.

Fig. 6(a) shows that the distribution of amplitude is almost uniform when the channel is relatively stable in case 1. Fig. 6(b) shows that when Rx is close to Tx, the amplitude of the positive part is higher than the negative part generally and it reaches highest at **7.324Hz**, which is the Doppler frequency required and basically consistent with theoretical result, **8Hz**. While in case 3, when Rx is away from Tx, as shown in Fig. 6(c), opposite to case 2, the negative part is much higher and it reaches highest at **-8.887Hz**, also close to inferred **-8Hz**.

Comparing Fig. 6(b) and Fig. 6 (c), it could be observed that the amplitude is higher in case 3 than in case 2 generally, and the gap between the positive part and negative part is more obvious in case 3. The reason might be the higher SNR, for shorter distance between Tx and Rx in the beginning which means less noise.

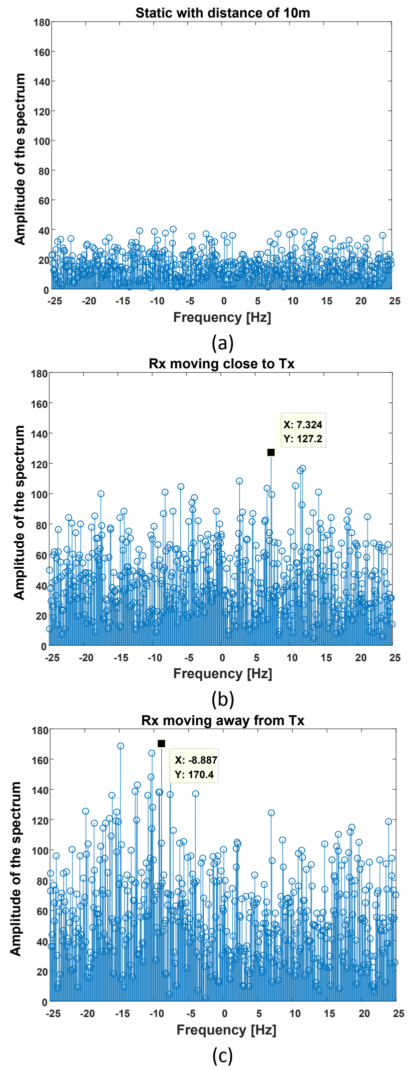


Figure 6. Spectrum diagram of three cases.

## VI. Conclusion

This paper proposes a method to measure Doppler shift in indoor corridors using WiFi and theoretically analyses the principle of Doppler shift measurement based on CSI. Utilizing the CSI acquisition system we built, experiments of three cases are conducted in a corridor and results proved the effectiveness of theoretical analysis. The method proposed in this paper could help measure the real Doppler frequency containing the speed and direction, it could be applied in related human detection.

## Acknoledgement

This work is supported by NSFC 61671011, 61401266, 61501289.

## REFERENCES


[1] E. Cianca, M.D. Sanctis and S.D. Domenico, “Radios as Sensors”, IEEE Internet of Things Journal, 2017, vol. 4, no. 2, pp. 363-373.

[2] T. Yoshida and Y. Taniguchi, “Estimating the number of people using existing wifi access point in indoor environment”, in Proceedings of the 6th European Conference of Computer Science (ECCS '15) pp. 46-53.

[3] S. Depatla, A. Muralidharan and Y. Mostofi, “Occupancy Estimation Using Only WiFi Power Measurements”, IEEE Journal on Selected Areas in Communications, 2015, vol. 33, no. 7, pp. 1381-1393.

[4] W. Xi, J. Zhao, X.Y. Li, K. Zhao, S. Tang, X. Liu and Z.Jiang, “Electronic frog eye: Counting crowd using WiFi”, in IEEE INFOCOM 2014, pp. 361-369.

[5] S. D. Domenico, G. Pecoraro, E. Cianca, and M. D. Sanctis, "Trained-once device-free crowd counting and occupancy estimation using WiFi: A Doppler spectrum based approach." in 2016 IEEE 12th International Conference on Wireless and Mobile Computing, Networking and Communications (WiMob), pp. 1-8.

[6] Y. Wang, K. Wu, and L. M. Ni, “WiFall: Device-Free Fall Detection by Wireless Networks,” IEEE Transactions on Mobile Computing, vol. 16, no. 2, pp. 581-594, 2017.

[7] W. Wang, A. X. Liu, M. Shahzad, K. Ling, and S. Lu, “Device-Free Human Activity Recognition Using Commercial WiFi Devices,” IEEE Journal on Selected Areas in Communications, vol. 35, no. 5, 2017, pp. 1118-1131.

[8] D. Zhang, H. Wang, and D. Wu, “Toward Centimeter-Scale Human Activity Sensing with Wi-Fi Signals,” Computer, vol. 50, no. 1, 2017, pp. 48-57,.

[9] C. Feng, W. S. A. Au, S. Valaee, and Z. Tan, “Received-Signal-Strength-Based Indoor Positioning Using Compressive Sensing,” IEEE Transactions on Mobile Computing, vol. 11, no. 12, 2012, pp. 1983-1993.

[10] C. Wu, Z. Yang, Y. Liu, and W. Xi, “WILL: Wireless Indoor Localization without Site Survey,” IEEE Transactions on Parallel and Distributed Systems, vol. 24, no. 4, 2013, pp. 839-848.

[11] H. Lim, L. C. Kung, J. C. Hou, and H. Luo, “Zero-Configuration, Robust Indoor Localization: Theory and Experimentation.” IEEE INFOCOM 2006, pp. 1-12.

[12] D. Halperin, W. Hu, A. Sheth, and D. Wetherall, "Predictable 802.11 packet delivery from wireless channel measurements." in ACM SIGCOMM 2010 Conference, vol.40, no.4, pp. 159-170.

[13] IEEE Std. 802.11n-2009: Enhancements for higher throughput.